ELSEVIER

Journal of Fluids and Structures 18 (2003) 783–794

JOURNAL OF FLUIDS AND STRUCTURES

www.elsevier.nl/locate/jnlabr/yjfls

# Energy consideration of the nonlinear effects in a Rijke tube

K.I. Matveev*,[1]

*California Institute of Technology, Pasadena, CA 91125, USA*

Received 23 December 2002; accepted 1 July 2003

**Abstract**

The goal of this work is to characterize the excited states of a thermoacoustic system with mean flow. The properties of excited regimes are determined by the balance between thermoacoustic energy transformation and acoustic losses. In many systems, the sound intensity is not sufficient for nonlinear acoustic losses to be a major factor in defining nonlinear saturation of thermoacoustic instability. It is the nonlinearity of the heat transfer process that is responsible for limit-cycle stabilization of linearly unstable acoustic modes and for the appearance of higher harmonics. In the present study, both a nonlinear theory based on energy consideration and a model for the nonlinear convective heat transfer in unsteady flow are developed. Experimental data are obtained for the excited regimes of operation of an electric Rijke tube. Model results for hysteresis in the transition between stable and excited states and for limit-cycle parameters are compared with test data.


## 1. Introduction

Thermoacoustic instability can arise in chambers of thermal devices where heat release is unsteady. When heat addition fluctuates in phase with pressure perturbations, the instability is encouraged in accordance with Rayleigh criterion (Rayleigh, 1945). This phenomenon leads to excitation of acoustic eigenmodes. Thermoacoustic instability is utilized in thermoacoustic engines (Swift, 1988) and pulsed combustors (Bai et al., 1993), but it is undesirable in most industrial burners (Pun, 2001) and rocket motors (Culick, 1988), where thermal and acoustic pulsations degrade operational performance and increase emitted noise. The fundamental mechanisms of thermoacoustic instability can be studied using a Rijke tube, the simplest system exhibiting heat-driven acoustic oscillations. This device, first built by Rijke (1859), consists of a pipe (resonator) with a localized heat source and a mean flow. A vertically oriented Rijke tube is shown schematically in Fig. 1. At certain values of system parameters (gauze location, heat supplied, and flow rate), a high-intensity sound is generated.

An extensive review on Rijke devices is given by Raun et al. (1993). In order to eliminate some deficiencies of the previous studies of Rijke tubes, both a series of experiments, aimed at determining the stability boundary with specified data uncertainties, and a linear stability analysis, including the effects of temperature field nonuniformity, were carried out by Matveev and Culcik (2003). Within a linear model, however, it is impossible to explain the nonlinear properties of a Rijke tube, such as limit-cycle characteristics and hysteresis in the stability boundary. A theory for the nonlinear unsteady heat transfer from a cylinder in the Oseen limit of flow motion was developed by Bayly (1985). An analysis of the nonlinear acoustic effects in a Rijke tube was carried out by Heckl (1990); an empirical model for the nonlinear unsteady heat transfer rate was applied with coefficients selected to fit experimental findings. Yoon et al. (2001)

*Corresponding author.
*E-mail address:* matveev@lanl.gov (K.I. Matveev).
[1] Present address: MS K764, Los Alamos National Laboratory, Los Alamos NM 87545.

0889-9746/$ - see front matter © 2003 Elsevier Ltd. All rights reserved.
doi:10.1016/j.jfluidstructs.2003.07.016

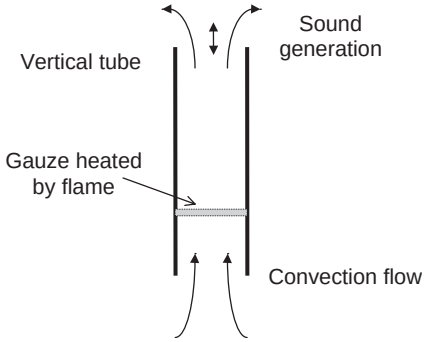


Fig. 1. Vertically oriented Rijke tube.

constructed the two-mode acoustic model for a duct with heat addition, using a phenomenological law for the thermal response of a concentrated heater to velocity fluctuations.

A nonlinear theory applicable for a wide range of Reynolds numbers (based on a diameter of the wire in the heating element) was introduced by Matveev and Culick (2002a). That approach, involving a finite-difference method of solving the wave equation in a media with a nonuniform temperature field, explained hysteresis and predicted the limit-cycle properties of a self-excited mode. In the present study, a model based on the energy consideration is developed with a primary objective to obtain analytical expressions for the limit-cycle characteristics of thermoacoustic devices. Although this model is less accurate than the previous approach (Matveev and Culick, 2002a), it is more convenient for fast estimation of the nonlinear regimes and for possible implementation of control means. Model results are compared with experimentally found characteristics of the unstable acoustic mode and excited higher harmonics in an electrically heated Rijke tube.

## 2. Theory

### 2.1. Linear model

Let us consider an idealized one-dimensional Rijke tube shown in Fig. 2. This is a pipe open at both ends with mean flow and a concentrated heat source, which is a permeable element heated electrically. The heat transfer from this element to the air-flow is of the forced convection type. All time-averaged properties of an air-flow are treated as constants along the tube. These properties are evaluated at the spatially averaged temperature $T$, which is a function of the flow rate and input power. A pressure drop over the tube is negligible. Acoustic oscillations are small in amplitude, allowing us to consider only linear effects. These oscillations are represented via longitudinal acoustic eigenmodes. Deviation of the excited mode frequencies from corresponding natural frequencies is ignored. Both thermoacoustic energy input and acoustic losses do not significantly affect the ideal mode shapes. The thickness of the heating element is much smaller than the acoustic wavelength. Gravity and other body forces are neglected. Gas flow speed is small compared to the speed of sound.

The linear wave equation approximates pressure perturbations in the air-flow inside the Rijke tube:

$$\frac{\partial^2 p'}{\partial t^2} + \zeta\frac{\partial p'}{\partial t} - a^2\frac{\partial^2 p'}{\partial x^2} = (\gamma - 1)\frac{\partial \dot{q}'}{\partial t}, \tag{1}$$

where $\zeta$ is the generic damping, $a$ is the speed of sound, $\gamma$ the gas constant, and $\dot{q}'$ is the rate of unsteady heat addition to the air-flow per unit volume. Pressure perturbation is considered via decomposition on acoustic eigenmodes (Culick, 1976):

$$p' = \sum_{n=1}^{N} p'_n = p_0 \sum_{n=1}^{N} \eta_n(t)\psi_n(x), \tag{2}$$

where $p_0$ is the mean pressure and $\eta_n(t)$ and $\psi_n(x)$ are the time-varying amplitude and the mode shape of the $n$th mode. Mode shapes are found from the undisturbed homogeneous wave equation:

$$\frac{\partial^2 p'}{\partial t^2} - a^2\frac{\partial^2 p'}{\partial x^2} = 0. \tag{3}$$

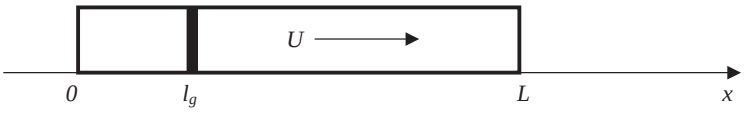


Fig. 2. One-dimensional Rijke tube with a concentrated heat source.

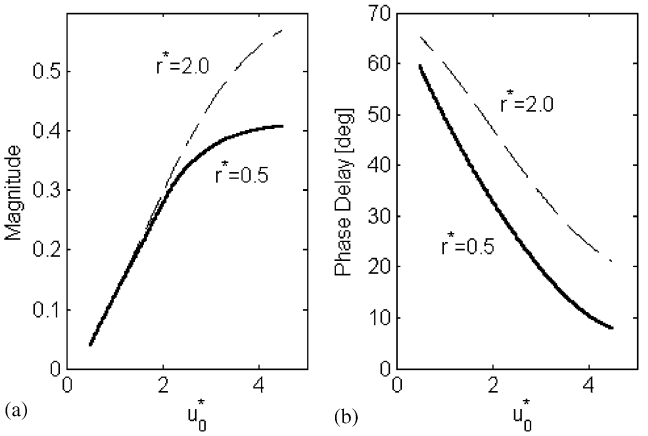


Fig. 3. Magnitude and phase delay of the transfer function.

The tube ends are considered to be open, hence the boundary conditions are

$$p'|_{x=0} = p'|_{x=L} = 0, \tag{4}$$

where $L$ is the effective tube length. The orthogonal mode shapes can be determined from Eqs. (2)–(4):

$$\psi_n(x) = \sin(k_n x), \tag{5}$$

where $k_n = \omega_n/a$ is the wavenumber and $\omega_n = \pi n a/L$ is the natural frequency of the $n$th mode.

The system stability can be found from the stability of individual modes: if at least one mode is unstable, then the system is unstable. Stability of an individual mode is determined by the net energy addition to this mode. Modes can be considered separately; we assume that they are linearly uncoupled. Thermoacoustic energy converted from the heat to the $n$th acoustic mode per one cycle of oscillation can be found as follows (Culick, 1976):

$$\Delta E_{n,\text{added}} = \frac{(\gamma-1)S}{\gamma p_o}\int_0^L \mathrm{d}x \int_0^\tau p_n' \dot{q}' \,\mathrm{d}t, \tag{6}$$

where $S$ is the cross-sectional area of the tube and $\tau$ is the cycle period.

Total heat addition rate $\dot{Q}(t)$ to the air-flow is conditioned by the heat transfer from the heating element. Since this heat transfer depends on the Reynolds number, the unsteady part of heat addition (per unit volume) in low Mach number flows in a linearized form is proportional to the velocity fluctuation $u'$ (Merk, 1957):

$$\dot{q}' = \frac{\dot{Q}_0}{S}\mathrm{Tr}_{\text{lin}}\frac{u'}{u_0}\delta(x-l_g), \tag{7}$$

where $\dot{Q}_0$ is the mean (time-averaged) heat addition rate, $u_0$ is the mean flow velocity; $l_g$ is the heater location and $\delta$ is the delta function (heater is assumed to be infinitely thin). The coefficient $\mathrm{Tr}_{\text{lin}} = |\mathrm{Tr}_{\text{lin}}|\exp(-\mathrm{i}\varphi)$ is the linear heat transfer function; in linear regimes $|u'| \ll u_0$. In our system the heater consists of a mesh of thin wires, and we apply the results of a numerical study for the unsteady heat release from a cylinder in a cross-flow (Kwon and Lee, 1985), taking into account a finite amplitude of velocity fluctuation in the referenced numerical study. The transfer function magnitude $|\mathrm{Tr}_{\text{lin}}|$ and phase delay $\varphi$ are shown in Fig. 3 as functions of nondimensional parameters $u_0^* = u_{0,\text{eff}}/\sqrt{\omega\chi}$ and $r^* = r\sqrt{\omega/\chi}$, where $u_{0,\text{eff}}$ is the effective mean flow velocity accounting for a partial blockage by the heater components, $r$ is the wire radius, and $\chi$ is the thermal diffusivity. The magnitude of the transfer function approaches zero at low mean flow velocities. The phase shift, necessary for thermoacoustic energy conversion, tends to zero at high

values of the mean flow velocity. That means there should be an intermediate range of flow velocities favourable for instability excitation. This is in accordance with test results on the stability boundary (e.g. Raun et al., 1993; Matveev and Culcik, 2003).

The acoustic velocity is related to the pressure perturbation as $u' = ip'_x/\omega\rho_0$. Time-varying amplitude of the $n$th mode is assumed to have form $\eta_n(t) = A_n \sin(\omega_n t)$. Substituting Eqs. (2) and (7) into (6), and integrating over a chamber volume and a cycle period, we find that thermoacoustic energy added to the $n$th mode during one cycle of oscillation is

$$\Delta E_{n,\text{added}} = \frac{\gamma-1}{\gamma}\frac{\pi}{2}\frac{|\text{Tr}_{\text{lin}}|\dot{Q}_0 p_0 S A_n^2}{am\omega_n}\sin(\varphi_n)\sin(2\,k_n l_g), \tag{8}$$

where $m$ is the mass flow rate and $\varphi_n$ is the phase delay of the transfer function corresponding to the $n$th mode. Since the phase shift is always less than $90^\circ$ in our system, a sign of the added energy is determined by the last multiplier in Eq. (8), which in turn is dependent on the mode number and a heater location. From this equation, it directly follows that the first mode can be excited if the heater is in the upstream half of the tube; the positions of the heater favourable for the second mode instability are the first and the third quarter of the tube; and so on for higher modes. This is in accordance with all previous experimental studies, e.g. Rijke (1859) and Raun et al. (1993), as well as the present investigation.

The loss of acoustic energy during one cycle of oscillation is due to the acoustic boundary layer on the tube walls and sound radiation from the open tube ends. These components are calculated with standard approximate expressions (e.g. Howe, 1998):

$$\Delta E_{n,\text{bl}} = \frac{\pi}{2\sqrt{2}}\frac{p_0 \Pi L A_n^2}{\gamma\sqrt{\omega_n}}\left(\sqrt{\nu}+(\gamma-1)\sqrt{\chi}\right), \tag{9}$$

$$\Delta E_{n,\text{sr}} = \frac{1}{2}\frac{\omega_n p_0 S^2 A_n^2}{\gamma a}, \tag{10}$$

where $\Pi$ is the perimeter of a tube cross-section, and $\nu$ is the kinematic viscosity. By using Eq. (10) we assume that wavelength is large compared to the tube diameter; that is valid for low acoustic eigenmodes. When the Mach number of the mean flow is high enough, the mechanism of acoustic power loss due to convection may become important (Ingard and Singhal, 1975). Since we consider only low Mach number flows, this effect can be neglected in this study.

At fixed heater location and mass flow rate, the onset of thermoacoustic instability occurs when the input electric power $P$ becomes sufficiently high, making thermoacoustic energy addition, Eq. (8), equal to the acoustic energy losses, found from Eqs. (9) and (10). A part of the electric power $P$ is not delivered to the air-flow, because of the heat conduction through insulation frame to the tube walls and thermal radiation. The relation between $P$ and $\dot{Q}_0$ will be given later in the experimental section of this paper.

### 2.2. Nonlinear model

The goal of this section is to derive a reduced-order model that approximates major nonlinear mechanisms with a purpose of predicting the properties of excited states of a Rijke tube. The possible causes for saturating the limit cycle of a linearly unstable mode are nonlinear gasdynamics effects at high amplitudes of acoustic oscillations, nonlinear boundary conditions at the tube edges due to flow separation, and a nonlinear character of the heat transfer process. Matveev and Culick (2002a) have established that the first two effects are very weak in our system due to low Mach number flows ($M \sim 10^{-3}$) and a given geometry, so these mechanisms cannot limit sound amplitudes at the levels found during the tests. However, in the systems with different specifications, it is possible to have a situation when nonlinear losses play an important role in determining the saturation of acoustic instability, such as in the study by Heckl (1990).

During the tests in our system, it was observed that the oscillating velocity amplitude (estimated in the heater vicinity) tends to stabilize near the mean flow velocity, slightly exceeding it. This observation shows that an appearance of the *flow reversal* at the heat source may be critical for nonlinear modelling of heat addition. Throughout this section we will use two additional assumptions: first, the coupling between acoustic modes due to nonideal boundary conditions, damping, and nonlinear acoustics is so small that it can be ignored; and second, each acoustic mode responds only to the forcing with a frequency close to its natural frequency.

The nonlinear transfer function Tr to be used for modelling the flows with a finite acoustic amplitude is defined as follows:

$$\dot{q}'_\omega = \frac{\dot{Q}_0}{S}\text{Tr}\frac{u'_\omega}{u_0}\delta(x-l_g), \tag{11}$$

where $f_\omega$ designates a component of the function $f$ oscillating with frequency $\omega$. A new hypothesis is invoked for a special form of Tr. It is assumed that the effects of a finite amplitude and a frequency can be separated:

$$\mathrm{Tr}(\omega,\alpha) = G(\alpha)\mathrm{Tr}_{\mathrm{lin}}(\omega), \tag{12}$$

where $G(\alpha)$ is the nonlinear correction to the transfer function; the nonlinear parameter $\alpha = (u_1'/u_0)_{x=lg}$ is the ratio of acoustic velocity amplitude to the mean flow velocity estimated at the heater plane. The specific form (12) is adopted to derive the nonlinear transfer function analytically. There is no underlying physics that can justify this assumption. However, this idea is somewhat similar to the method of describing functions successfully applied in the nonlinear control system theory (e.g. Eveleigh, 1972), where the output is assumed to be proportional to the input (the same frequency) with a coefficient depending on the oscillation amplitude.

To derive an expression for $G(\alpha)$, let us start from considering steady flow. The heat transfer rate valid for our system in this case has a form typical for convective heat transfer (Matveev and Culcik, 2003):

$$\dot{Q}^{st} = K\sqrt{u_0}, \tag{13}$$

where superscript *st* means steady and coefficient $K$ is proportional to the temperature difference between the air-flow and the heater. For the case of unsteady flow with an oscillating component having a very low frequency, the flow is in a quasi-steady regime. In this case, the momentary heat transfer rate can be computed using the formula valid for steady flow and substituting the instantaneous flow velocity into the right-hand side of Eq. (13). In the following derivation, we assume that the time-averaged (mean) heat transfer rates for the unsteady and quasi-steady regimes are equal.

Thus, the quasi-steady heat transfer rate can be approximated by a simple rule:

$$\dot{Q}^{qs}(t) = K\sqrt{|u(t)|}, \tag{14}$$

where superscript *qs* means quasi-steady and $u(t) = u_0 + u'(t)$ is the total flow velocity in the heater vicinity. Eq. (14) implies that the heat release does not depend on the flow direction and is determined only by a magnitude of the flow velocity. This form of the heat transfer rate is appropriate for typical Rijke tubes, where the temperature of the gas pockets that crossed the heater plane remains significantly lower than the heater temperature.

In principle, other forms for the quasi-steady heat release rate can be used. For example, in the situation where gas is heated nearly up to the temperature of the gauze, which could happen at sufficiently low flow rates, the heat transfer rate can be taken equal to zero during time intervals when the total velocity at the heater is negative, i.e., when flow reversal occurs. A more sophisticated approach would introduce a reduction of the heat release rate proportional to the reduction in temperature difference between gas and a hot grid. In this case, flow pockets must be traced in space and time, and the heat release rate would become a complicated function of time due to sinusoidal variation of the flow velocity, a nonlinear form of the heat transfer rate, and multiple crossing of the heater plane by flow particles. For clarity of the mathematical formulation, we decided to use the simplest form for the quasi-steady heat transfer rate, Eq. (14), that should help explain the major nonlinear characteristics of a Rijke tube.

Notice that in the regime approaching a quasi-steady case, the time delay induced by the transfer function tends to zero. As follows from definitions introduced in the previous section, $r^* \to 0$ and $u_0^* \to \infty$ as $\omega \to 0$. In these limits, as can be seen in Fig. 3b, the phase delay $\varphi$ goes to zero. Therefore, Eqs. (11) and (14) are compatible.

As follows from Eqs. (7) and (14), $\mathrm{Tr}_{\mathrm{lin}}^{qs} = \frac{1}{2}$ in the linear quasi-steady regime; therefore, from Eq. (12) we obtain $G(\alpha) = 2\mathrm{Tr}^{qs}(\alpha)$. The nonlinear quasi-steady transfer function $\mathrm{Tr}^{qs}$ can be found using Eqs. (11) and (14) and assuming a sinusoidal function for the oscillating velocity component $u'(t) = u_0\alpha\sin(\omega t)$:

$$\frac{\dot{Q}_\omega^{qs}(t)}{\dot{Q}_0^{qs}} - 1 = \mathrm{Tr}^{qs}\alpha\sin(\omega t). \tag{15}$$

Taking a Fourier component corresponding to the frequency $\omega$, we find the nonlinear correction $G(\alpha)$:

$$G(\alpha) = \frac{4}{\alpha\tau}\int_0^\tau \left(\frac{\dot{Q}_\omega^{qs}(t)}{\dot{Q}_0^{qs}} - 1\right)\sin(\omega t)\,\mathrm{d}t. \tag{16}$$

The computed dependence of $G(\alpha)$ on the nonlinear parameter is shown in Fig. 4a. Notice that $G(0) = 1$, i.e., $\mathrm{Tr}^{qs}(\alpha) \to \frac{1}{2}$ as $\alpha \to 0$. When the nonlinear parameter significantly exceeds unity, the nonlinear transfer function monotonically decreases; hence, further development of thermoacoustic instability is discouraged. This property causes saturation of the limit cycles deep in the excited regimes.

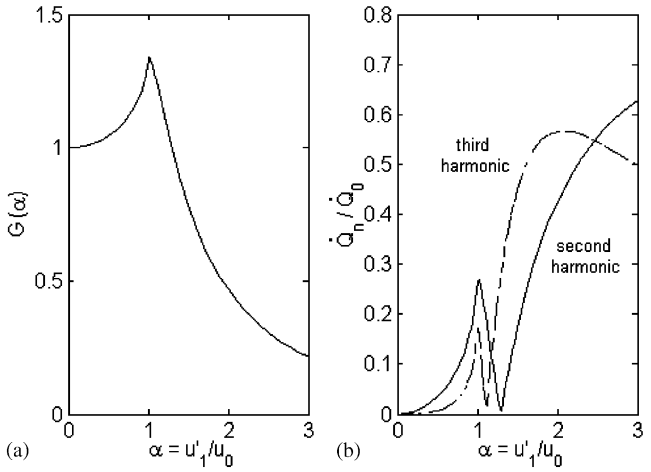


Fig. 4. (a) Nonlinear correction for heat transfer function and (b) amplitudes of higher harmonics of heat addition.

The fact that $G(\alpha)$ increases at small amplitudes of the acoustic velocity is due to the nonlinear form of the quasi-steady heat release rate (Eq. (14)). The mean heat transfer rate $\dot{Q}_0^{qs}$ decreases in the range $0<\alpha<1$ (no flow reversal yet). The transfer function Tr is proportional to the ratio between the unsteady and mean components of the heat transfer rate; this results in the increase of $G(\alpha)$ in this interval of nonlinear parameter $\alpha$. A physically similar dependence was derived by Bayly (1985) in the limit of the small Peclet number based on the wire radius.

Nonmonotonic behaviour of $G(\alpha)$ in the range $0<\alpha<2$ leads to the remarkable results. The magnitude of the transfer function affects the effectiveness of the thermal-to-acoustic energy conversion (Eq. (8)): the larger the transfer function, the more significant is the unsteady component of the heat transfer rate. Due to nonmonotonic shape of the nonlinear transfer function, the same energy input into the acoustic mode can occur for more than one value of the amplitude of acoustic oscillations. This energy addition compensates acoustic losses, and hence, leads to the existence of the equilibrium limit cycles. Initially, the transfer function grows with increasing amplitude of the acoustic velocity fluctuation; therefore, the linearly stable system may also have two excited equilibrium states: one corresponds to the inclining part of the transfer function curve ($0<\alpha<1$) and the other to the declining portion ($\alpha>1$). The equilibrium limit cycle, corresponding to the increasing branch of Tr, is unstable, because at a small deviation from this point the increment of thermoacoustic energy conversion has a sign opposite to that needed to return the system into the equilibrium state. Another equilibrium limit cycle, corresponding to the declining branch of Tr, is stable, since in this case the energy input to the acoustic mode varies in the way to prevent a deviation from the equilibrium point. Because of the existence of multiple equilibrium states in the vicinity of the stability boundary, the system condition is dependent on the history of parameter variation; this phenomenon is identified as hysteresis.

Due to a nonlinear character of the heat transfer, an oscillatory flow produces higher harmonics in the heat release. The amplitudes of these harmonics can be computed by formula:

$$\dot{Q}_n = \frac{2}{\tau}\left|\int_0^{\tau} \dot{Q}^{qs}(t)\exp(\mathrm{i}n\omega t)\mathrm{d}t\right|. \tag{17}$$

Higher harmonics of heat addition can excite higher acoustic eigen modes of the system. The amplitudes $\dot{Q}_n(\alpha_1)$ of the second and third harmonics are depicted in Fig. 4b as functions of the nonlinear parameter $\alpha_1$ of the first mode.

Thus, we identified a dominant mechanism that saturates limit cycles and determined the nonlinear correction to the heat transfer function. The amplitude of the unstable mode in excited regimes can be evaluated from Eqs. (8)–(10), similar to the linear case, but with corrected transfer function. We will assume here that only the first mode can be self-excited, which is relevant to our experimental configuration. However, the same theory is applicable for the cases when higher modes are linearly unstable. An implicit equation for the nonlinear parameter $\alpha_1$, corresponding to the equilibrium limit cycle of the first mode, is the following:

$$G(\alpha_1) = m\frac{\pi\Pi La\sqrt{\omega_1}\left(\sqrt{\nu}+(\gamma-1)\sqrt{\chi}\right)+\sqrt{2}\omega_1^2 S^2}{\sqrt{2}(\gamma-1)\pi|\mathrm{Tr}_{\mathrm{lin}}|\dot{Q}_0 S\sin\varphi_1\sin(2k_1 l_g)}. \tag{18}$$

The complex-valued amplitude of this mode is determined from the definition of the nonlinear parameter and the acoustic velocity mode shape:

$$A_1 = -\mathrm{i}\alpha_1 \frac{u_0 \gamma k_1^2}{\omega_1} \left( \frac{\mathrm{d}\psi_1}{\mathrm{d}x}(l_g) \right)^{-1}. \tag{19}$$

Due to nonlinearity of the heat transfer process, higher harmonics in the heat release appear when one mode becomes unstable and oscillates with a finite amplitude. These harmonics, having amplitudes computed by Eq. (17), drive higher acoustic modes, since the frequencies of heat release components are close to the natural frequencies of acoustic modes; in our idealized model these frequencies match exactly. Energy input into the $n$th mode caused by this phenomenon can be found by substituting Eq. (17) into (6):

$$\Delta E_{n,\mathrm{nonl}} = \frac{\gamma - 1}{\gamma} \frac{\pi \dot{Q}_n(\alpha_1) A_n}{\omega_n} \sin(k_n l_g). \tag{20}$$

The resulting amplitude of the $n$th mode is determined from energy balance:

$$\Delta E_{n,\mathrm{added}} + \Delta E_{n,\mathrm{nonl}} = \Delta E_{n,\mathrm{bl}} + \Delta E_{n,\mathrm{sr}}, \tag{21}$$

where energy inputs are evaluated by Eqs. (8)–(10) and (20). Substituting these formulae into (21), we can find the $n$th mode amplitude as a function of nonlinear parameters of the first and $n$th modes:

$$A_n = \frac{B_n \dot{Q}_n(\alpha_1)}{C_n - D_n G(\alpha_n)}, \tag{22}$$

where

$$B_n = 2\sqrt{2}\pi(\gamma - 1) am \sin(k_n l_g), \tag{23}$$

$$C_n = \pi p_0 \, am \Pi L \sqrt{\omega_n} \left( \sqrt{\nu} + (\gamma - 1)\sqrt{\chi} \right) + \sqrt{2} p_0 \, m \omega_n^2 S^2, \tag{24}$$

$$D_n = \sqrt{2}\pi(\gamma - 1) p_0 \, |\mathrm{Tr}_{\mathrm{lin}}| \dot{Q}_0 S \sin(\varphi_n) \sin(2k_n l_g). \tag{25}$$

To calculate the amplitudes of acoustic modes in the unstable regimes of operation of the Rijke tube, first, the amplitude of the self-excited mode is computed by Eq. (18), and then, higher mode amplitudes are found by solving Eq. (22) iteratively.

## 3. Experimental set-up

The experimental Rijke tube system employed in our study is schematically depicted in Fig. 5. The important elements of the system are outlined in this section; more detailed information can be found elsewhere (Matveev and Culcik, 2003). The horizontally oriented Rijke tube is a square aluminium tube of $9.5 \times 9.5$ cm cross-section and length 1.0 m. Mean air-flow is provided by a blower. A damping chamber, located between the tube and blower, prevents the influence on the blower from tube acoustics. The flow direction is from right to left.

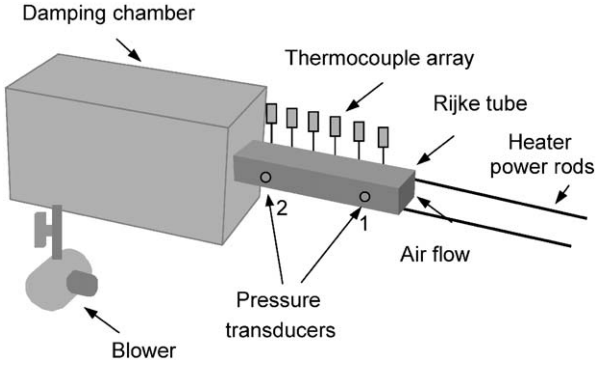


Fig. 5. Schematic view of experimental set-up.

The heat source is a nichrome grid with a wire diameter of 0.01 in. It is suspended on a macor frame and connected to the power source via copper rods. The power source consists of two TCR-20T250 power supplies, each capable of producing 500 amps of current. Heater position can be easily changed within the tube, even though in this study we use only one location of one quarter of the tube length from the upstream end.

The mean air-flow through the Rijke tube is provided by a GAST R1102 blower, with a maximum throughput of $0.0127\,m^3/s$ at standard conditions. The blower is operated at full capacity with a 2 in. by-pass ball valve controlling the amount of air drawn through the damping chamber. The flow rate is measured using a laminar flow element (Meriam 50MW20) and a differential pressure transducer (Honeywell Microswitch). This measurement takes place between the damping chamber and the blower.

The pressure transducers used were PCB model 112A04, coupled with a 422D11 charge amplifier and a 482A20 signal conditioner. Charge-mode piezoelectric transducers were utilized, since the majority of the electronics is located in a separate charge amplifier, increasing the operating temperature range while retaining relatively high sensitivities. The two pressure transducers, flush mounted in the tube at positions $x/L = 0.15$ and 0.80, are labelled 1 and 2, respectively (Fig. 5).

The data acquisition system is based on a Pentium III 700 MHz computer. A Computer Boards' CIO-DAS1602/12 data acquisition board is installed in the machine. In this configuration, data could be acquired in short bursts at over 8000 Hz, and for extended periods of time streaming to the hard drive at over 4000 Hz. For this configuration of the Rijke tube, the frequency of the self-excited mode is approximately 180 Hz, and the frequencies of two higher harmonics are about 360 and 540 Hz. These frequencies are easily captured at the rates capable by the data acquisition system.

An array of 15 thermocouples is suspended from the top of the tube to the centre-line. Thermocouples are used solely for time-averaged temperature measurements. Not all electric power supplied to the heater is delivered to the air-flow; a significant portion is lost via heat conduction to the tube walls and via thermal radiation. Complicated numerical heat transfer analysis, generating a temperature field inside the Rijke tube and the heat fluxes, has been developed by Matveev and Culick (2002b). In this study, we use correlations for the spatially averaged temperature $T$ and for the mean heat transfer rate $\dot{Q}_0$ from the heater to the air-flow as functions of the electric power input $P$ and the mean mass flow rate $m$:

$$T = T_0 + b_1 P^{b_2} \exp(-b_3 m), \tag{26}$$

$$\dot{Q}_0 = c_1 P^{c_2}(1 - \exp(-c_3 m)), \tag{27}$$

where the numerical values of power $P$ in Watts and mass flow rate $m$ in gm/s are substituted into the right-hand side of Eqs. (26) and (27). Coefficients have the following values: $T_0 = 300$, $b_1 = 0.579$, $b_2 = 0.849$, $b_3 = 0.189$, $c_1 = 2.07$, $c_2 = 0.805$, and $c_3 = 1.01$. Dimensions of the temperature $T$ and the heat transfer rate $\dot{Q}_0$ are degrees Kelvin and Watts, respectively. Relations (26) and (27) are purely empirical and not based on any physical model. The general form is chosen to satisfy asymptotic limits, and the coefficients are selected to minimize correlation errors within the range of system parameters typical for conditions studied.

## 4. Results

In the present study, one of the primary system parameters, the heater location, is kept fixed. The heating element is placed inside the pipe at one quarter of the tube length as measured from the upstream end. This position is the most favourable for excitation of thermoacoustic instability, and hence, the most convenient for studying the unstable regimes and the nonlinear effects. Test data and model results are reported for pressure fluctuation measured at location $\frac{3}{20}$ of the tube length from the upstream end; one of the pressure transducers was mounted there during the tests. Temperature field varies insignificantly with power and flow rate at this position for various system conditions. Although the selected location is not very far from the tube edge, no efforts were made to estimate the possible influence of the tube end effects on test results.

Let us first look at the history-dependent phenomena observed in the experiments and predicted by the model. Test data, typical for the transition to instability at high flow rates, are shown in Fig. 6a. We define the critical power as a power value at which the jump occurs from one state (stable or excited) to the other. A large gap is discovered between the critical powers that correspond to the opposite directions of power variation. This effect is identified as hysteresis at the stability boundary. Although not shown in the figure, there is also a stable zero-amplitude state on a lower side of the hysteresis loop, corresponding to the power increase up to 585 W where the transition to the excited state occurs. The choice of a particular state within the hysteresis loop is determined by the history of parameter variation.

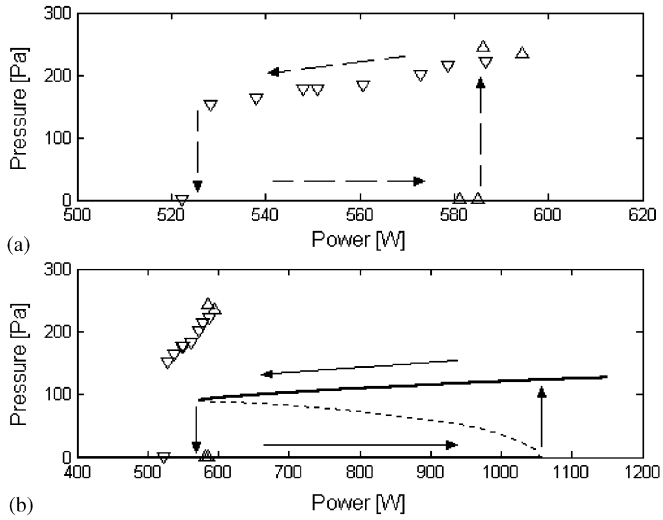


Fig. 6. Limit-cycle amplitudes of the first mode: (a) test data (△ power increase, ▽ power decease); (b) test data and model results (bold lines, stable limit cycles; dashed line, unstable). Mass flow rate 2.75 gm/s. Arrows show the direction of sound amplitude variation with changing power input: dashed arrows, test; solid arrows, model.

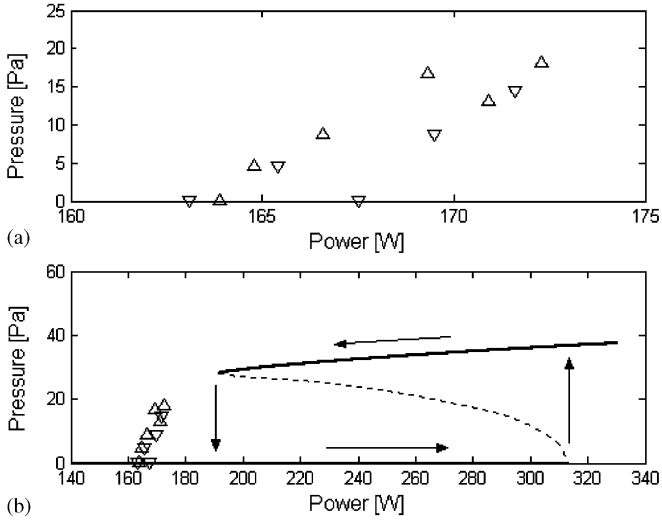


Fig. 7. Limit-cycle amplitudes of the first mode: (a) test data (△ power increase, ▽ power decease); (b) test data and model results (bold line, stable limit cycle; dashed line, unstable). Mass flow rate 0.89 gm/s.

The results obtained by modelling show a qualitatively similar pattern (Fig. 6b), though a quantitative agreement with test data is not achieved. The nonmonotonic shape of the transfer function, discussed in Section 2.2, can lead to the presence of three equilibrium limit cycles for the same values of the major system parameters. These limit cycles predicted by the model are manifested in Fig. 6b in the power range from 570 to 1060 W. One stable state has a zero amplitude; the second equilibrium is unstable and depicted by a dotted line; and the third equilibrium limit cycle is stable with an amplitude near 100 Pa. The horizontal dimension (power) of the calculated hysteresis loop is significantly larger than that measured; and the vertical size (sound amplitude) of the predicted loop is smaller than that obtained in the test.

At low-mass flow rates, experimental findings demonstrate a different pattern. History-dependent effects are not observed. In a certain power range, there is a regime that cannot be classified as either stable or excited, because sound sporadically appears and disappears. In Fig. 7a this regime corresponds to the interval 165–170 W; the records captured

within this range are arbitrary. The model still generates hysteresis (Fig. 7b). Notice that the experimental transition to instability and a modelled hysteresis loop do not overlap in this case. Possible reasons for this inconsistency in predicting the critical power at low flow rates are higher temperature gradients in the system, more significant contribution from natural convection at the gauze, and an increased role of air leakages in other system components.

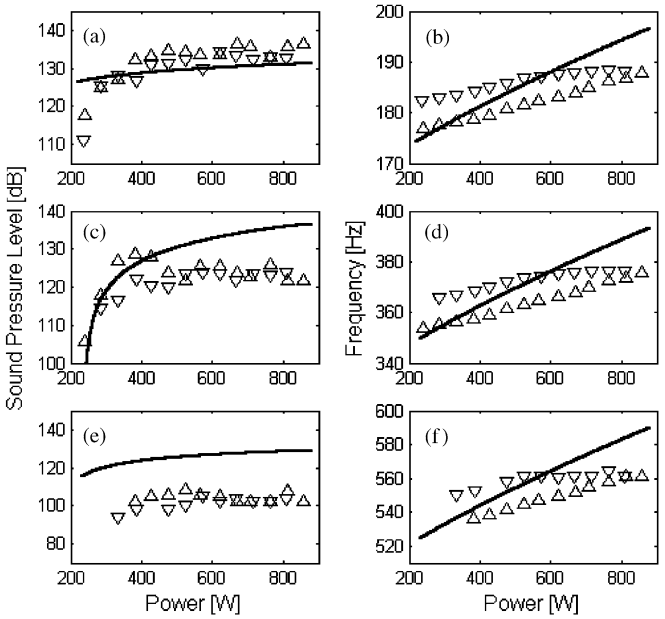


Fig. 8. Sound pressure level and frequency of acoustic modes. Mass flow rate 1.63 gm/s. (a), (b) First mode; (c), (d) second mode; (e), (f) third mode. Solid lines, model results; test data: △ power increase, ▽ power decrease.

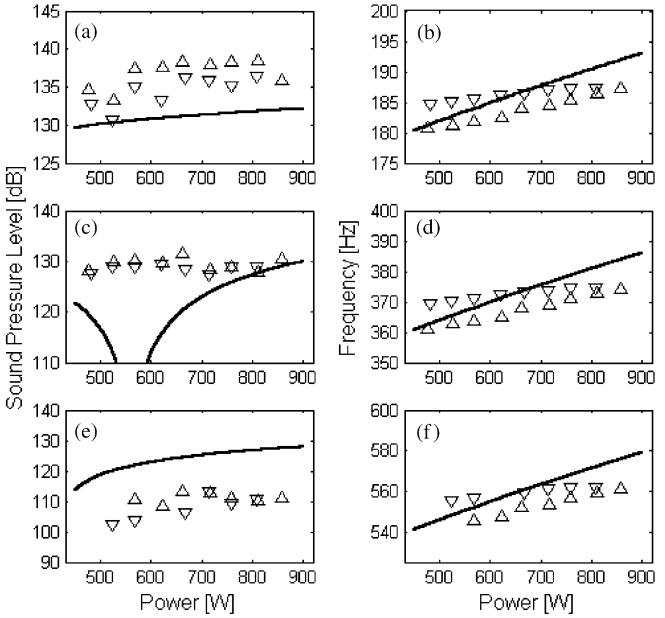


Fig. 9. Sound pressure level and frequency of acoustic modes. Mass flow rate 2.40 gm/s. (a), (b) First mode; (c), (d) second mode; (e), (f) third mode. Solid lines, model results; test data: △ power increase, ▽ power decrease.

The theory developed here helps to explain hysteresis in the stability boundary, although it overpredicts the gap between critical power values. We believe that the most likely cause for this discrepancy is a noise component in the air-flow. Variations of the flow rate even in stable regimes are around 10% (Matveev and Culcik, 2003). Those perturbations may be caused by the system structural elements disturbing the flow, such as the heater and the sharp edges of the tube entrance; also, fluctuations in the air sucked from outside the tube may be important. The presence of noise may trigger early transitions between stable and excited states. This mechanism would explain the overprediction of the observed gap between critical powers, corresponding to the opposite directions of power variation at high-mass flow rates (Fig. 6b). At low flow rates, the relative noise component in the flow rate is larger than that at high flow rates; also, the predicted hysteresis loop is smaller. These two effects combined can make the hysteresis phenomenon disappear, similar to experimental observations (Fig. 7a).

Now we look at the properties of the excited regimes of the Rijke tube far from the stability boundary. Experimentally and numerically found amplitudes and frequencies of the first three acoustic modes is given in Figs. 8 and 9 for two mass flow rates 1.63 and 2.40 gm/s. An agreement between calculated and measured amplitude of the first mode is acceptable. The amplitude of the second mode is computed satisfactorily only for some values of the system parameters. Due to the nonmonotonic behaviour of the heat release harmonics that drive higher acoustic modes, a drop in the amplitude of the second mode is predicted near 200 W for the first flow rate; this is in agreement with the test data. For the second flow rate, this dip appears near 550 W, that does not correlate with experimental results. The amplitude of the third mode is significantly overpredicted.

Thus, the theory developed here can be applied for quantitative estimation of the amplitude of the first self-excited mode and for qualitative assessment of the second harmonic in the unstable regimes of operation of a Rijke tube. Possible reasons for compromising the accuracy of higher mode prediction are the major model assumptions, such as a simple model for the heat transfer process at the presence of finite-amplitude velocity fluctuations (Eqs. (12), (14) and (17)), a disregard of mode shape distortion induced by temperature gradients, and a neglect of the damping chamber influence on the tube acoustics.

The mode frequencies presented in Figs. 8 and 9 are computed as functions of the system geometry and one variable parameter, spatially averaged temperature (Eq. (26)). Frequencies of higher harmonics are multiple integers of the first-mode frequency. This simple approach to determine the mode frequencies in the excited regimes of operation gives satisfactory agreement with experimental data. The rate of increase of modelled frequencies with heater power appears to be higher than that in the test. One of the reasons is the temperature field nonuniformity in a real situation that modifies natural frequencies. Also, frequencies observed in the limit cycles usually do not exactly coincide with natural frequencies; in this work, nonlinear factors are not accounted for calculating frequency correction.

## 5. Concluding remarks

In order to explain nonlinear effects of an electric Rijke tube, a simple theory is constructed using an energy approach. The equilibrium states of the system are found by balancing thermoacoustic energy input and acoustic losses. The excited regimes of this device are studied experimentally for one heater location and for variable power input and flow rate. The limit cycles of the acoustic modes are computed and compared with experimental data. To validate the general applicability of this theory, nonlinear effects should be studied at other heater locations, including those where higher eigenmodes cause the transition to instability. Such work is in progress and will be a subject of a later publication.

The ideas and methods discussed in this paper provide a better understanding of thermoacoustic instabilities. It is found that nonlinearity of unsteady heat transfer is a dominant factor in limiting limit-cycle saturation in our system. Nonlinear acoustic losses may become important, if sound intensity can reach higher values. The hysteresis effect in the stability boundary, characteristic for many thermal systems with unsteady heat release, is explained by the nonmonotonic behaviour of the heat transfer function. Analytical framework derived in this work allows for quantitative prediction of the properties of a linearly unstable mode deep in the excited regimes of operation of a Rijke tube and for qualitative estimation of higher modes.

Possible directions for future work include studying systems with more complicated heat addition mechanisms (e.g. combustion in burners) and noncompact heat sources (e.g. stacks in thermoacoustic engines). Detailed investigation of the heat transfer in pulsating flows, employing both experiments and CFD methods, would be an important step in improving the model accuracy. Application of active control techniques can be conveniently studied using a Rijke tube as the simplest thermoacoustic device.

**Acknowledgements**

The author would like to thank Professor Fred Culick of the California Institute of Technology for helpful discussions and support.

## References

Bai, T., Cheng, X.C., Daniel, B.R., Jagoda, J.I., Zinn, B.T., 1993. Performance of a gas burning Rijke pulse combustor with tangential reactants injection. Combustion Science and Technology 94, 1–10.

Bayly, B.J., 1985. Heat transfer from a cylinder in a time-dependent cross flow at low Peclet number. The Physics of Fluids 28, 3451–3456.

Culick, F.E.C., 1976. Nonlinear behavior of acoustic waves in combustion chambers, Parts I and II. Acta Astronautica 3, 714–757.

Culick, F.E.C., 1988. Combustion instabilities in liquid-fuelled propulsion systems—an overview. AGARD-CP-450.

Eveleigh, V.W., 1972. Introduction to Control System Design. McGraw-Hill, New York.

Heckl, M.A., 1990. Non-linear acoustic effects in the Rijke tube. Acustica 72, 63–71.

Howe, M.S., 1998. Acoustics of Fluid-Structure Interactions. Cambridge University Press, Cambridge.

Ingard, U., Singhal, V.K., 1975. Effect of flow on the acoustic resonances of an open-ended duct. Journal of the Acoustical Society of America 58, 788–793.

Kwon, Y.-P., Lee, B.-H., 1985. Stability of the Rijke thermoacoustic oscillation. Journal of the Acoustical Society of America 78, 1414–1420.

Matveev, K.I., Culcik, F.E.C., 2003. A study of the transition to instability in a rijke tube with axial temperature gradient. Journal of Sound and Vibration 264, 689–706.

Matveev, K.I., Culick, F.E.C., 2002a. Modeling of unstable regimes in a Rijke tube. In: Proceedings of the Fifth International Symposium on Fluid-Structure Interactions, ASME paper IMECE 2002-33369.

Matveev, K.I., Culick, F.E.C., 2002b. Experimental and mathematical modeling of thermoacoustic instabilities in a Rijke tube. 40th Aerospace Sciences Meeting and Exhibit, AIAA paper No. 2002-1013.

Merk, H.J., 1957. Analysis of heat-driven oscillations of gas flows. Applied Scientific Research A6, 402–420.

Pun, W., 2001. Measurements of thermo-acoustic coupling. Ph.D. Dissertation, California Institute of Technology.

Raun, R.L., Beckstead, M.W., Finlinson, J.C., Brooks, K.P., 1993. A review of Rijke tubes, Rijke burners and related devices. Progress in Energy and Combustion Science 19, 313–364.

Rayliegh, J.W.S., 1945. The Theory of Sound. Dover Publications, New York (re-issue).

Rijke, P.L., 1859. Notiz über eine neie art, die luft in einer an beiden enden offenen röhre in schwingungen zu versetzen. Annalen der Physik 107, 339–343.

Swift, G.W., 1988. Thermoacoustic engines. Journal of the Acoustical Society of America 84, 1145–1180.

Yoon, H.-G., Peddieson, J., Purdy, K.R., 2001. Non-linear response of a generalized Rijke tube. International Journal of Engineering Science 39, 1707–1723.